Betweenness centrality in multiplex brain network during mental task evaluation

Vladimir V. Makarov,[1] Maxim O. Zhuravlev,[1] Anastasija E. Runnova,[1] Pavel Protasov,[1] Vladimir A. Maksimenko,[1] Nikita S. Frolov,[1] Alexander N. Pisarchik,[1,2] and Alexander E. Hramov[1,3,*]

[1]*Yuri Gagarin State Technical University of Saratov, Politechnicheskaya str., 77, Saratov, 410054, Russia*
[2]*Technical University of Madrid, Campus Montegancedo, E-Madrid 28223, Spain*
[3]*Saratov State University, Astrakhanskaya str., 83, Saratov, 410012, Russia*

(Received 22 August 2018; revised manuscript received 30 October 2018; published 26 December 2018)

In this paper we study the structural properties of a functional network of the human brain during the evaluation of mental tasks using the concept of betweenness centrality. We carry out the experiments involving the alternating trials of mental task evaluation with simultaneous registration of electroencephalographic (EEG) data. Using the wavelet phase coherence we reconstruct the functional multiplex network of the brain considering the different typical frequency bands of EEG activity as interconnected layers. We reveal that transition from a resting state to evaluation of a cognitive task leads to the strong outflow of shortest paths from low frequencies and strengthening of high-frequency connectivity in the brain. At the same time, we observe that mental activity shapes the shortest paths in a more uniform distribution across the brain, which implies the emergence of a more distributed functional network. Our results are in good agreement with recent studies of cognitive activity and can be implied in the design of brain-computer interfaces for the estimation of cognitive load or attention.

DOI: 10.1103/PhysRevE.98.062413

I. INTRODUCTION

The processes underlying cognitive functions are of a great interest in modern neuroscience [1,2]. The close attention of researchers to this topic is caused not only by the urge to reveal the fundamental aspects of brain behavior. Recent studies show the strong possibility of early diagnosis of mental disorders [3] and mild cognitive impairments [4,5] using analysis of electrical brain activity during the evaluation of various mental tasks. At the same time, efficient classification and scoring of mental activity can be used in a variety of brain-computer interface (BCI) applications with neurofeedback [6], which present themselves as a promising technology for research in many related fields of cognitive science [7].

The considerable progress in the investigation of cognitive activity has been made using electroencephalographic (EEG) frequency analysis. In particular, the importance of alpha (8–12 Hz) and theta (4–8 Hz) bands has been shown in several studies [8,9].

In Ref. [10] the strong increase of spectral power in the gamma (40–80 Hz) band is shown during the performance of eight types of mental tasks with the task-related differences. Brouwer *et al.* develop an algorithm for estimation of cognitive load using the event-related potentials and spectral power of EEG signals [11].

However, the recent focus of studies has drifted to the complex network approach of the analysis of mental activity and cognitive performance [12,13]. All types of the highest nervous activity are accompanied by strong interaction between various regions of the brain [14]. The measurement of this interaction allows us to access the functional network of the brain corresponding to the specific state or activity, which, in turn, can be utilized to reveal the principles underlying this activity [15]. Using modern techniques for brain activity recording, one can represent functional brain structure as a graph, where separate nodes are brain areas, whose temporal dynamics is described by a signal from a particular sensor, and edges indicate the presence of a functional relation between brain areas (nodes). Recent research shows that cognitive load expresses itself as specific connectivity patterns, distinct in various frequency scales of brain electrical activity [16–18].

In this paper we study the structural properties of a functional network of the human brain during the evaluation of mental tasks using the concepts of multiplexing and betweenness centrality [19]. First, in term of multiplexing concept, we decompose functional brain structure into multiple layers, where each layer reflects brain behavior in a particular frequency band. Second, our choice of betweenness centrality as a network characteristic is motivated by two main reasons. On the one hand, we want to quantify the interplay between functional network layers corresponding to different frequency bands, and the contribution of each one of them into the specific brain activity. On the other hand, we are eager to understand which parts of each layer are involved in the interlayer cooperation. For this reason we are measuring the *betweenness centrality* as the quantity which can estimate the importance of the node as a pacemaker in both intra- and interlayer connections. For example, the eigenvector centrality will allow us only to score the importance of layers in a multiplex network [20], while the intralayer ranking will be implied by the layer with the highest algebraic connectivity [21].

We carry out a number of experiments, in which participants were solving training tests on visual perception with parallel registration of surface EEG recordings. It should be noted that each recording contained the active (task evaluation) and passive (rest) trials. Using the wavelet phase coherence [22,23] we estimate the functional connectivity matrices for each trial in six typical EEG frequency bands:

*hramovae@gmail.com

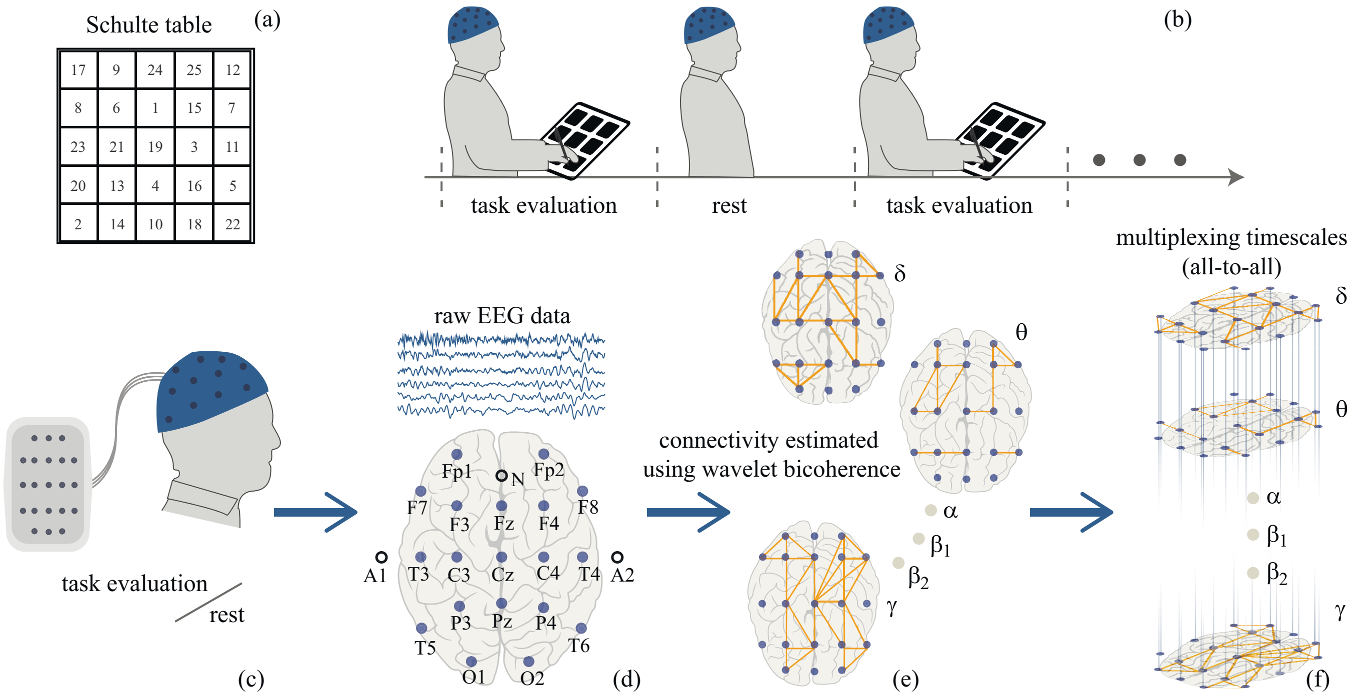

FIG. 1. (a) The depiction of an example of the Schulte table. (b) Principal design of the experiment on Schulte table evaluation. (c)–(f) The procedure of the reconstruction of the functional multiplex network (see text for details).

delta ($\delta = 0.5$–4 Hz), theta ($\theta = 4$–8 Hz), alpha ($\alpha =$ 8–12 Hz), beta-1 ($\beta_1 = 12$–25 Hz), beta-2 ($\beta_2 = 25$–40 Hz), and gamma ($\gamma = 40$–80 Hz), which present themselves as a classical segmentation of EEG spectra [24]. As soon as we wanted to catch the structural properties of the whole functional network, we arranged the obtained structures in the multiplex network [25], where each node is connected to itself in each other layer (EEG frequency bands); i.e., each node is characterizing the dynamics of a specific brain region in the specific frequency band. Next, we measure betweenness centrality of each node to reveal the influence of cognitive load on the distribution of shortest paths inside and among the layers of a functional multiplex network of the brain.

We reveal that transition from resting state to evaluation of a cognitive task leads to the strong outflow of shortest paths from low frequencies and strengthening of high-frequency connectivity in the brain. At the same time, we observe the redistribution of betweenness centrality in each particular layer or frequency range. More specifically, the mental activity shapes the shortest paths in a more uniform distribution across the brain, which implies the emergence of a distributed functional network binding the areas of the brain with dynamical interactions. Our results are in a good agreement with recent studies of mental activity [26–28] and can be used both in fundamental studies and in practical implications involving the design of BCIs for measuring and controlling attention and/or cognitive load [29].

II. METHODS

A. Experimental design

The experiments were carried out during the first half of the day at a specially equipped laboratory where the volunteer was sitting comfortably and effects of external stimuli, e.g., external noise and bright light, were minimized. The $S = 8$ subjects performed a series of attentional tests using the Schulte table. The Schulte table represents a square matrix with five columns and five rows, in which numbers from 1 to 25 are placed in random order [see Fig. 1(a)]. The volunteer is asked to search for numbers in ascending order (from 25 to 1) and point to them in the table using a pen. The experiment for each subject [see Fig. 1(b)] contained $M = 5$ active stages (Schulte table evaluation), which were alternating with the passive stages (rest).

During all experiments, the multichannel EEG data have been acquired using the BE Plus LTM amplifier (EB Neuro S.P.A., Florence, Italy). Data were recorded at an 8 kHz sampling rate using the standard bipolar method of registration with two reference and $N = 19$ electrodes [see Fig. 1(d)]. The adhesive Ag/AgCl electrodes based in special prewired head caps were used to obtain the EEG signals. Two reference electrodes, A1 and A2, were located on mastoids, while the ground electrode N was located above the forehead. The EEG signals were filtered by a bandpass filter with cutoff points at 1 Hz (HP) and 300 Hz (LP) and a 50-Hz Notch filter. To accurately split the recording into the active (Shulte table evaluation) and passive (rest) phases we used the video recording during all stages of the experiment.

Subjects participated in the experiment on a voluntary and gratuitous basis. All participants signed an informed medical consent to participate in the experimental work and received all necessary explanations about the process, including their agreement for further publication of the results. Acquired experimental data were processed with respect for the confidentiality and anonymity of research respondents. The experimental studies were performed in accordance with the

Declaration of Helsinki and approved by the local research Ethics Committee of the Yuri Gagarin State Technical University of Saratov.

B. Reconstruction of multiscale connectivity

We use the wavelet bicoherence to estimate the strength of interaction between the brain regions. The wavelet bicoherence has proved itself to be very powerful instrument to quantify the interactions on various scales of biological systems [22,30,31], including brain activity [32,33]. Below a detailed description of the calculation of wavelet bicoherence for the pairs of EEG signals is presented.

We calculate the complex-valued wavelet coefficients $W_i(f,t_0)$ for each EEG channel $x_i(t)$ as

$$W_i(f,t_0)=\sqrt{f}\int_{t_0-4/f}^{t_0+4/f}x_i(t)\psi^*(f,t-t_0)dt, \tag{1}$$

where $i=1,\dots,N$ is the number of the considered EEG channel, $N=19$ is the total number of EEG channels, t_0 specifies the wavelet location on the time axis and the asterisk denotes the complex conjugation, and $\psi(f,t)$ is the mother wavelet function. We use the Morlet wavelet, which is often utilized for processing of biological signals [22],

$$\psi(f,t-t_0)=\sqrt{f}\pi^{-1/4}e^{i\omega_0 f(t-t_0)}e^{-f^2(t-t_0)^2/2}, \tag{2}$$

where ω_0 is the wavelet scaling parameter and i is an imaginary unit. Previously we found that parameter $\omega_0=2\pi$ in the continuous wavelet transform provides an optimal time-frequency resolution of EEG signal [34,35].

To measure the degree of coherence between two EEG signals $x_i(t)$ and $x_j(t)$, we use the corresponding complex-valued wavelet coefficients $W_i(f,t)=a_i+ib_i$ and $W_j(f,t)=a_j+ib_j$.

Wavelet bicoherence, $\sigma_{ij}(f,t)$, is estimated based on the mutual wavelet spectrum $W_{i,j}(f,t)$ of the signals $x_i(t)$ and $x_j(t)$. Similarly to Ref. [36] the coefficients $\mathrm{Re}[\sigma_{ij}(f,t)]$ and $\mathrm{Im}[\sigma_{ij}(f,t)]$ represented as real and imaginary parts of mutual wavelet spectrum can be calculated via Eqs. (3) and (4), respectively:

$$\mathrm{Re}[\sigma_{ij}(f,t)]=\frac{a_i(f,t)a_j(f,t)+b_i(f,t)b_j(f,t)}{\sqrt{a_i^2(f,t)+b_i^2(f,t)}\sqrt{a_j^2(f,t)+b_j^2(f,t)}} \tag{3}$$

and

$$\mathrm{Im}[\sigma_{ij}(f,t)]=\frac{b_i(f,t)a_j(f,t)-a_i(f,t)b_j(f,t)}{\sqrt{a_i^2(f,t)+b_i^2(f,t)}\sqrt{a_j^2(f,t)+b_j^2(f,t)}}. \tag{4}$$

Next, we evaluate the degree of coherence between the different EEG signals, recorded during each EEG trial of rest or evaluation of cognitive task for each subject p. The values were averaged over time intervals involved in each trial of the experiment. As a result, time-averaged coefficients $\mathrm{Re}[\sigma_{ij}(f)]_{T_{mp},m,p}$ and $\mathrm{Im}[\sigma_{ij}(f)]_{T_{mp},m,p}$ were obtained as

$$\mathrm{Re}[\sigma_{ij}(f)]_{T_{mp},m,p}=\frac{1}{MS}\sum_{p=1}^{S}\sum_{m=1}^{M}\frac{1}{T_{mp}}\int_{T_{mp}}\mathrm{Re}[\sigma_{ij}(f,t)]dt \tag{5}$$

and

$$\mathrm{Im}[\sigma_{ij}(f)]_{T_{mp},m,p}=\frac{1}{MS}\sum_{p=1}^{S}\sum_{m=1}^{M}\frac{1}{T_{mp}}\int_{T_{mp}}\mathrm{Im}[\sigma_{ij}(f,t)]dt, \tag{6}$$

where $M=5$ is the number of stages of cognitive task evaluation or rest, S is the number of subjects, and T_{mp} is the duration of the mth stage of task evaluation by the pth subject determined by recorded video analysis or the duration of the rest interval which was fixed at $T_{mp}=10$ s. Based on coefficients (5) and (6), the degree of coherence, $\sigma(f)$, between the EEG signals was estimated as the amplitude of the mutual wavelet spectrum:

$$\sigma_{ij}(f)=\sqrt{\{\mathrm{Re}[\sigma_{ij}(f)]_{T_{mp},m,p}\}^2+\{\mathrm{Im}[\sigma_{ij}(f)]_{T_{mp},m,p}\}^2}. \tag{7}$$

The $\sigma_{ij}(f)$ function takes values from 0 to 1, containing the information about the degree of phase coherence of the two signals $x_i(t)$ and $x_j(t)$ for the particular frequency. There $\sigma_{ij}(f)=0$ implies that there is no phase coherence at the current frequency, for $\sigma_{ij}(f)>0$ partial coherence takes place and $\sigma_{ij}(f)=1$ indicates complete coherence.

Obtained values (7) were then averaged over EEG frequency bands. As the result, coefficients $\sigma_{ij}(s)$ defined the coherence between EEG signals in six typical EEG frequency bands ($\Delta f=\delta,\theta,\alpha,\beta_1,\beta_2,\gamma$):

$$\sigma_{ij}(\Delta f)=\frac{1}{\Delta f}\int_{\Delta f}\sigma(f)df. \tag{8}$$

C. Network analysis

Using the wavelet bicoherence between the pairs of channels $i,j=1,\dots,N$ we reconstruct the $\sigma_{ij}(\Delta f)$ coupling matrices in six considered frequency bands ($\Delta f=\delta,\theta,\alpha,\beta_1,\beta_2,\gamma$) [see Fig. 1(e)] for each $p=1,\dots,S$ subject's stage of the experiment for the task evaluation stages (ESs) and for the stages of rest (RSs). It should be noted that by definition of the wavelet coherence measure σ the signals are self-correlated, so the elements of the main diagonal $\sigma_{ii}(\Delta f)=1$.

Due to the aspects of the betweenness calculation in the weighted networks [19], more specifically, while the weight is considered as a distance, we should make the inverse transformation of each adjacency matrix:

$$w_{ij}(\Delta f)=1-\sigma_{ij}(\Delta f), \tag{9}$$

and thus we have the inverse values within the range of [0,1].

To reveal the features of interaction between different timescales of neuronal activity during cognitive load we arrange the connectivity structures $w_{ij}(\Delta f)$ obtained for each

Frequency band, Δf, in the multiplex network [Fig. 1(f)]:

$$\Omega = \begin{bmatrix} w_{ij}(\delta) & E & E & E & E & E \\ E & w_{ij}(\theta) & E & E & E & E \\ E & E & w_{ij}(\alpha) & E & E & E \\ E & E & E & w_{ij}(\beta_1) & E & E \\ E & E & E & E & w_{ij}(\beta_2) & E \\ E & E & E & E & E & w_{ij}(\gamma) \end{bmatrix}, \tag{10}$$

where E is an identity matrix. It should be noted that in this process each node (corresponding to the specified EEG channel) becomes connected to itself in all other layers (EEG frequency bands). The magnitude of the interlayer links is not chosen randomly: while the value of $w_{ij}(\Delta f)$ is always less than 1, although it can be very close to it, the shortest paths between the nodes located in the same layer will preferably go through that layer.

Since we have obtained the final network structure, we are able to calculate the betweenness centrality for the each node, g_i, corresponding to the ith EEG channel:

$$g_i = \sum_{i \neq j \neq k} \frac{\Lambda^i_{jk}}{\Lambda_{jk}}, \tag{11}$$

where Λ^i_{jk} is the number of shortest paths between node j and k which pass through node i, and Λ_{jk} is the total number of shortest paths between j and k. We use the algorithm for weighted networks proposed in Ref. [19] and calculate the values for the each node of the multiplex network (10). After that we normalize the betweenness centrality of each node on the total value in the multiplex network:

$$g'_i = \frac{g_i}{\sum_{i=1}^{6N} g_i}. \tag{12}$$

III. RESULTS

To get insight into the interplay between the timescales of neuronal dynamics we will first investigate the integral value of the betweenness of each layer during the resting state and mental tasks. For this purpose we summarize the values of betweenness in each layer and represent the final quantity as a percentage of the total in the multiplex network:

$$G(\delta) = \sum_{i=1}^{N} g_i, \quad G(\theta) = \sum_{i=1+N}^{2N} g_i,$$
$$G(\alpha) = \sum_{i=1+2N}^{3N} g_i, \quad G(\beta_1) = \sum_{i=1+3N}^{4N} g_i, \tag{13}$$
$$G(\beta_2) = \sum_{i=1+4N}^{5N} g_i, \quad G(\gamma) = \sum_{i=1+5N}^{6N} g_i;$$

i.e., we calculate the relative number of shortest paths going through each layer.

The corresponding values for task and rest stages each gathered from 40 sample multiplex networks are shown in Fig. 2. One can easily see that the resting state is characterized by the dominance of lower frequencies. The median value of delta range betweenness centrality takes more than 30%, theta range and alpha range take around 20%, and none of the high-frequency bands demonstrate a median value more than 10%. We should note the high variance of betweenness in the resting state, which is conditioned by very individual differences between the subject's neuronal activity during passive wakefulness [37]. However, during the evaluation cognitive task the distribution of betweenness in frequency ranges drastically changes. The first thing which arrests our attention is the strong narrowing of the boxes. This fact demonstrates that person's concentration on the strictly formalized task such as Schulte table solving leads to emergence of similar functional connectivity patterns considering both different trials and subjects. Here we can see the very different distribution of betweenness among frequency ranges in comparison to the resting state: median values for each timescale lie in range 10%–20%, and the delta and gamma bands demonstrate very similar values. The delta frequency range has dropped its betweenness greatly together with the theta range, while the alpha band shows a small decrease of betweenness. At the same time, the sufficient amount of shortest paths is now going through the high frequencies. We can track a strong increase of betweenness for all three ranges, beta-1, beta-2, and gamma, but the gamma band seems the most dominant among them.

To gain a deeper insight into the connectivity features during the transition from resting state to cognitive load we investigate the betweenness values for each node in the

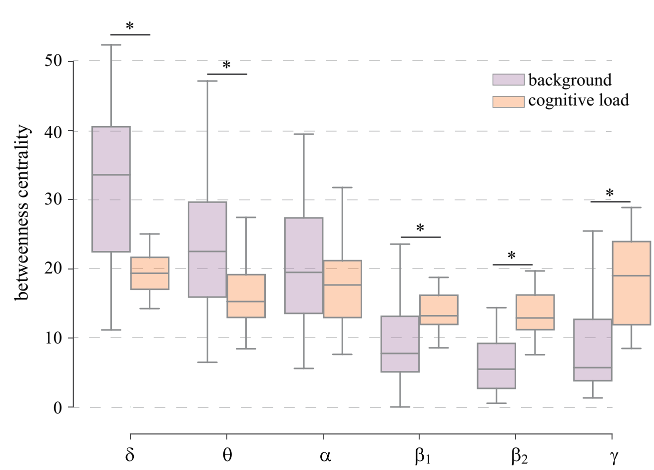

FIG. 2. The relative value of betweenness centrality, which share each frequency band in a multiplex network for passive (purple) and active (orange) phase of the experiment are shown via box plots.

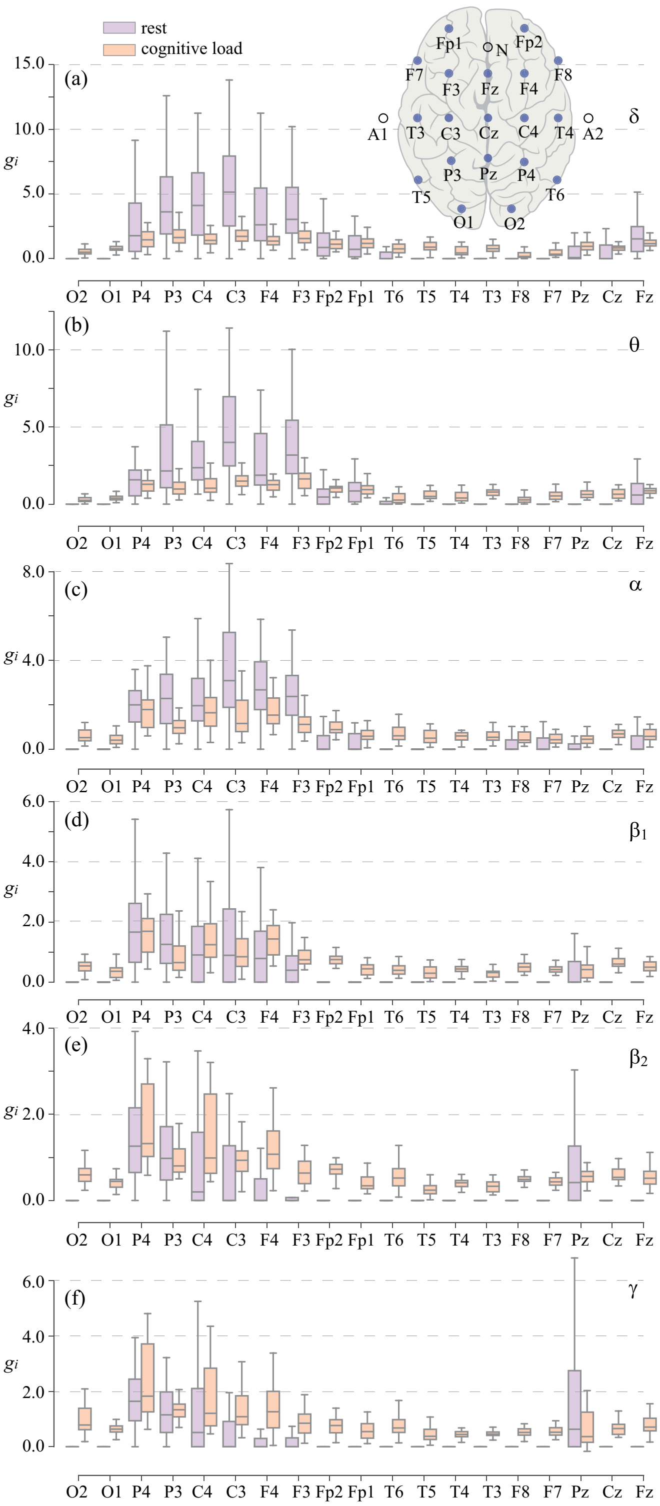

FIG. 3. The relative value of betweenness centrality for each channel in the (a) delta, (b) theta, (c) alpha, (d) beta-1, (e) beta-2, and (f) gamma range for the passive (purple) and active (orange) phase of the experiment are shown via box plots.

network. Figure 3 shows separate plots for the each frequency band, displaying each channel's betweenness centrality. Here we can observe that the in resting state the majority of shortest paths are concentrated across the parietal and frontal lobes (P4, P3, C4, C3, F4, F3). An interesting fact is that the channels Pz (except the high frequencies), Cz, and Fz (i.e., channels across longitudinal fissure) do not exhibit high values of betweenness here, while they are located right inside this region. This behavior manifests itself across all frequency bands i.e., layers of the network. The latter is also caused by a dominance of the specific layer in the network (in our case the delta range), which redistributes the shortest paths according to its structure [38]. Some differences between layers still can be observed as some redistribution of paths in the parietal and frontal lobes.

The crucial differences between the frequency bands reveal themselves, and then we proceed to the analysis of the active stage of experiment, i.e., the evaluation of the cognitive task. We can see the emergence of an almost uniform distribution of betweenness in the delta and theta ranges, caused by a decrease of values corresponding to P4, P3, C4, C3, F4, and F3 together with visible increase of betweenness of the temporal (T3, T4, T5, T6), occipital (O1, O2), and frontal (F5, F6) lobes, which is presented in all frequency ranges. In the alpha and beta-1 ranges the betweenness of channels P4, P3, C4, C3, F4, and F3 does not demonstrate pronounced changes, while in high-frequency beta-2 and gamma ranges it has grown significantly. In fact, we can observe the gradual transition from a sharp decrease of betweenness across the parietal and frontal lobes (P4, P3, C4, C3, F4, F3) in the delta range to a pronounced increase of this value in the gamma range. Notably, it is also results in a homogeneous distribution of betweenness centrality over EEG channels of betweenness in low frequencies, i.e., delta and theta ranges.

We can track the mentioned changes in detail by plotting the change in betweenness centrality spatially across the brain (see Fig. 4). For this reason we calculate the following quantity for each node in the multiplex network:

$$\varepsilon_i = g_i^{ES} - g_i^{RS}, \tag{14}$$

i.e., the average difference in the amount of shortest paths going through the specific node in the task evaluation (g_i^{ES}) and rest (g_i^{RS}) stages of experiment. It should be noted that nodes belonging to different layers exhibit the various amplitude of changes. For example, the ε_i for the delta range demonstrates the larger magnitude due to its strong connectivity in the resting state. The box plot, which allows us to evaluate this disparity, is shown in Fig. 4(a).

In the delta range [Fig. 4(b)] we can observe an almost equal decrease of betweenness in both hemispheres together with its increase across the longitudinal fissure. The latter effect is also pronounced in the theta and alpha ranges and could be a marker of the strengthening of interhemispherical interaction during the cognitive load in low frequencies. At the same time, changes in the theta, alpha, and beta-1 ranges do not demonstrate hemispherical symmetry [Figs. 4(c)–4(e)]; here we can observe much more sufficient decrease in the left hemisphere, which drifts from the frontal (F3) to parietal (P3) lobe during the transition from the theta to beta-1 range. This process is accompanied by the increase of betweenness in the frontal cortex in high frequencies. However, the number of shortest paths in the prefrontal cortex, associated with decision-making patterns, grows in all frequency ranges. Since the solving of the Schulte table is strongly connected

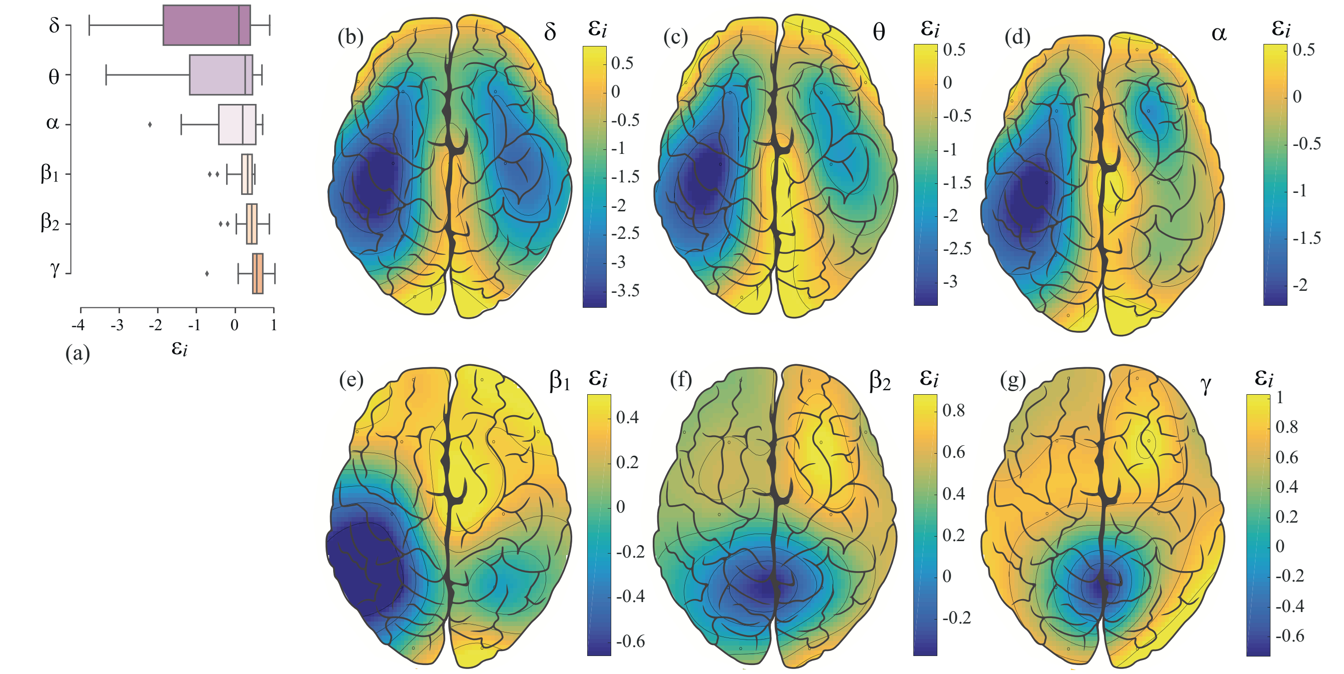

FIG. 4. The box plot (a) and spatial distributions (b)–(g) of the ε quantity (see text for definition) for the (b) delta, (c) theta, (d) alpha, (e) beta-1, (f) beta-2, and (g) gamma frequency ranges.

with visual perception, we can observe the strong increase of connectivity in the visual cortex during the evaluation of this task. In the gamma range the betweenness centrality grows in all areas of the neural network except the Pz channel [Fig. 4(g)]. In fact, we can easily track the competitive interplay between the structural properties of low- and high-frequency functional networks.

We also check if this behavior is related to the processes of the cognitive load, and not linked to motor activity and visual coordination, which are involved during the evaluation of the Schulte table. For this reason we have carried out a series of experiments in which participants were asked to point randomly on an empty whiteboard every 5 s (5 s passive stage, 5 s active stage, eight participants). Due to the short duration of the active phases, their number was increased to 10 for each participant. The corresponding comparison of betweenness centrality distribution over frequency bands for motor action and evaluation of the Shulte table is shown in Fig. 5. One can see that in the case of motor tasks the structural features of the multiplex network are much more similar to the passive phase (see Fig. 2 for comparison) and characterized by the dominance of low frequencies. This observation bolsters our conclusion that cognitive load is linked to the increase of functional connectivity in the high-frequencies range of brain activity.

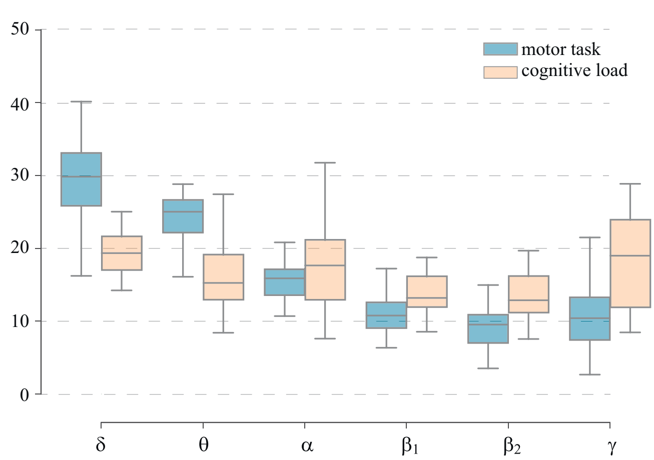

FIG. 5. The relative value of betweenness centrality, which share each frequency band in a multiplex network during the motor task (blue), and the evaluation of the Schulte table (orange) are shown via box plots.

IV. DISCUSSION AND CONCLUSIONS

Summing up our study, we have analyzed the evolution of connectivity patterns, namely, the distribution of shortest paths, in the brain functional network during the transition from resting state to cognitive task evaluation. We can observe the gradual transition from a sharp decrease of betweenness across the parietal and frontal lobes (P4, P3, C4, C3, F4, F3) in the delta range to a pronounced increase of these values in the gamma range. Such dynamics is accompanied by an increase of betweenness in the brain areas associated with visual information processing and decision making.

What can it tell us about the processes of brain activity during cognitive load? Certainly, we can observe the emergence of strong interaction in high frequencies such as the beta-2 and gamma range, the effect well correlated with present research on attentional and cognitive processes in the brain [10]. At the same time, we can see that such activity strongly affects the overall connectivity of the neural network and shapes the shortest paths in a more uniform distribution, caused by the increase of connectivity in the temporal (T3, T4, T5, T6),

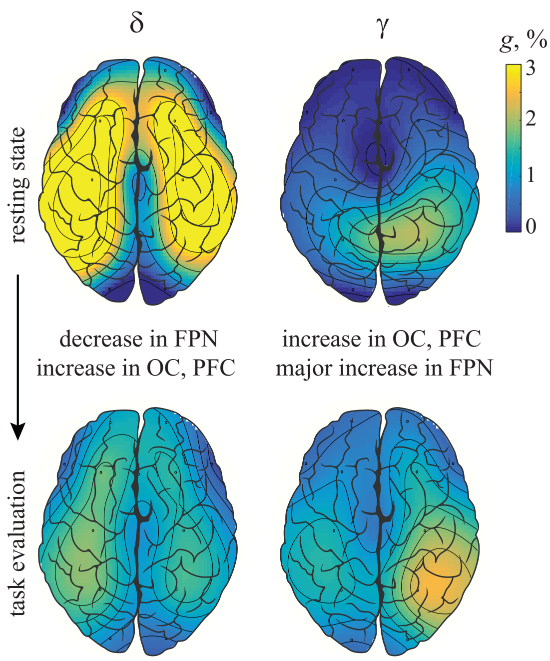

FIG. 6. The spatial distributions of betweenness centrality in the delta and gamma range in transition from a resting state to task evaluation. Here FPN = frontoparietal network, OC = occipital cortex, PFC = prefrontal cortex.

occipital (O1, O2), frontal (F5, F6), and prefrontal (Fp1, Fp2) lobes. To get a clear representation of this process, we have depicted the spatial maps of betweenness centrality in the delta and gamma ranges in Fig. 6. This behavior reveals that mental activity, such as evaluation of cognitive tasks, involves the emergence of a distributed functional network binding the areas of the brain with dynamical interactions. Such an effect is very consistent with Refs. [39,40], where authors show a correlation between efficiency of the resting state functional network and the person's IQ.

Our results are in good correspondence with the recent research on cognitive load: the emergence of gamma band oscillations across the brain during working memory load is also shown in Ref. [26] by analysis of intracranial EEG recordings. Similar to Ref. [27] where the authors use the features of functional network of mental task classification, we observe strong hemispherical asymmetry of alpha range connectivity involving the strengthening of the right hemisphere. The increase of beta range connectivity in the prefrontal and frontal lobe during perception and recognition is also shown in Ref. [28], whose authors examine functional networks built on the basis of wavelet bicoherence.

The strong involvement of the fronto-parietal network in cognitive task solving and working memory is known from recent fMRI studies. Lee and authors [41] compare the fMRI signals of adolescents during the evaluation of Raven Progressive Matrixes of various complexity. They have found that tasks with high complexity specifically increased regional activity in the bilateral fronto-parietal network, including the lateral prefrontal, anterior cingulate, and posterior parietal cortices. Harding and authors [42] have found that both cognitive control and working memory tasks activate the fronto-parietal network but in different connectivity configurations. In our study we have shown that activation of this area is directly connected with the high-frequency neural interaction in the gamma band (see Fig. 6 once again). The cognitive task evaluation is accompanied by strong information transfer through the gamma range all over the brain, in which the fronto-parietal network plays the role of a pacemaking hub [43].

Despite particular features of the network evolution, we can observe the strong interplay between the connectivity of high and low frequencies. This effect is most vividly pronounced if we consider the distributions for the delta and gamma ranges [see Figs. 4(b) and 4(g)]: during the transition from resting state to evaluation of cognitive task they demonstrate almost opposite changes. Such behavior once again supports the hypothesis of a competitive interaction between frequency scales of a neural network [44,45].

ACKNOWLEDGMENTS

We would like to express our gratitude to the reviewers for comments and suggestions that have improved the article. This work has been supported by the Russian Science Foundation (Project No. 17-72-30003) in the part "experimental study, estimation of brain connectivity and development of the multiplex network model for brain dynamics analysis." V.V.M., N.S.F., A.E.R., and A.E.H. thank the President Program (Projects No. MK-5850.2018.2 and No. NSH-2737.2018.2) in the part "neurophysiological big data processing."

[1] M. D'esposito and B. R. Postle, The cognitive neuroscience of working memory, Annu. Rev. Psychol. **66**, 115 (2015).

[2] R. A. Poldrack and T. Yarkoni, From brain maps to cognitive ontologies: Informatics and the search for mental structure, Annu. Rev. Psychol. **67**, 587 (2016).

[3] Y. Li, D. Cao, L. Wei, Y. Tang, and J. Wang, Abnormal functional connectivity of EEG gamma band in patients with depression during emotional face processing, Clin. Neurophysiol. **126**, 2078 (2015).

[4] S. Waninger, C. Berka, A. Meghdadi, M. S. Karic, K. Stevens, C. Aguero, T. Sitnikova, D. H. Salat, and A. Verma, Event-related potentials during sustained attention and memory tasks: Utility as biomarkers for mild cognitive impairment, Alzheimer's Dementia **10**, 452 (2018).

[5] H.-S. Chiang, R. A. Mudar, A. Pudhiyidath, J. S. Spence, K. B. Womack, C. M. Cullum, J. A. Tanner, J. Eroh, M. A. Kraut, and J. Hart Jr., Altered neural activity during semantic object memory retrieval in amnestic mild cognitive impairment as measured by event-related potentials, J. Alzheimer's Dis. **46**, 703 (2015).

[6] K.-S. Hong, N. Naseer, and Y.-H. Kim, Classification of prefrontal and motor cortex signals for three-class fNIRS-BCI, Neurosci. Lett. **587**, 87 (2015).

[7] C. Jeunet, B. NKaoua, S. Subramanian, M. Hachet, and F. Lotte, Predicting mental imagery-based BCI performance from personality, cognitive profile and neurophysiological patterns, PLoS ONE **10**, e0143962 (2015).

[8] W. Klimesch, EEG alpha and theta oscillations reflect cognitive and memory performance: A review and analysis, Brain Res. Rev. **29**, 169 (1999).

[9] B. Zoefel, R. J. Huster, and C. S. Herrmann, Neurofeedback training of the upper alpha frequency band in EEG improves cognitive performance, NeuroImage **54**, 1427 (2011).

[10] S. Fitzgibbon, K. Pope, L. Mackenzie, C. Clark, and J. Willoughby, Cognitive tasks augment gamma EEG power, Clin. Neurophysiol. **115**, 1802 (2004).

[11] A.-M. Brouwer, M. A. Hogervorst, J. B. Van Erp, T. Heffelaar, P. H. Zimmerman, and R. Oostenveld, Estimating workload using EEG spectral power and ERPs in the n-back task, J. Neural Eng. **9**, 045008 (2012).

[12] S. L. Bressler and V. Menon, Large-scale brain networks in cognition: Emerging methods and principles, Trends Cognit. Sci. **14**, 277 (2010).

[13] O. Sporns, Contributions and challenges for network models in cognitive neuroscience, Nat. Neurosci. **17**, 652 (2014).

[14] M. Rubinov and O. Sporns, Complex network measures of brain connectivity: Uses and interpretations, NeuroImage **52**, 1059 (2010).

[15] H.-J. Park and K. Friston, Structural and functional brain networks: from connections to cognition, Science **342**, 1238411 (2013).

[16] Z. Dai, J. De Souza, J. Lim, P. M. Ho, Y. Chen, J. Li, N. Thakor, A. Bezerianos, and Y. Sun, EEG cortical connectivity analysis of working memory reveals topological reorganization in theta and alpha bands, Front. Hum. Neurosci. **11**, 237 (2017).

[17] N. A. Crossley, A. Micheli, P. E. Vrtes, T. T. Winton-Brown, A. X. Patel, C. E. Ginestet, P. McGuire, and E. T. Bullmore, Cognitive relevance of the community structure of the human brain functional coactivation network, Proc. Natl. Acad. Sci. USA **110**, 11583 (2013).

[18] U. Braun, A. Schfer, H. Walter, S. Erk, N. Romanczuk-Seiferth, L. Haddad, J. I. Schweiger, O. Grimm, A. Heinz, H. Tost *et al.*, Dynamic reconfiguration of frontal brain networks during executive cognition in humans, Proc. Natl. Acad. Sci. USA **112**, 11678 (2015).

[19] U. Brandes, A faster algorithm for betweenness centrality, J. Math. Sociol. **25**, 163 (2001).

[20] J. Aguirre, D. Papo, and J. M. Buld, Successful strategies for competing networks, Nat. Phys. **9**, 230 (2013).

[21] L. Sol, M. Romance, R. Criado, J. Flores, A. Garca del Amo, and S. Boccaletti, Eigenvector centrality of nodes in multiplex networks, Chaos **23**, 033131 (2013).

[22] A. E. Hramov, A. A. Koronovskii, V. A. Makarov, A. N. Pavlov, and E. Sitnikova, *Wavelets in Neuroscience*, Springer Series in Synergetics (Springer, Heidelberg, 2015).

[23] V. A. Maksimenko, A. E. Runnova, N. S. Frolov, V. V. Makarov, V. O. Nedaivozov, A. A. Koronovskii, A. N. Pisarchik, and A. E. Hramov, Multiscale neural connectivity during human sensory processing in the brain, Phys. Rev. E **97**, 052405 (2018).

[24] R. Miller, Theory of the normal waking EEG: from single neurones to waveforms in the alpha, beta and gamma frequency ranges, Intl. J. Psychophysiol. **64**, 18 (2007).

[25] M. De Domenico, S. Sasai, and A. Arenas, Mapping multiplex hubs in human functional brain networks, Front. Neurosci. **10**, 326 (2016).

[26] M. W. Howard, D. S. Rizzuto, J. B. Caplan, J. R. Madsen, J. Lisman, R. Aschenbrenner-Scheibe, A. Schulze-Bonhage, and M. J. Kahana, Gamma oscillations correlate with working memory load in humans, Cereb. Cortex **13**, 1369 (2003).

[27] G. N. Dimitrakopoulos, I. Kakkos, Z. Dai, J. Lim, A. Bezerianos, Y. Sun *et al.*, Task-independent mental workload classification based upon common multiband EEG cortical connectivity, IEEE Trans. Neural Syst. Rehabilitation Eng. **25**, 1940 (2017).

[28] W. Jamal, S. Das, K. Maharatna, I. Pan, and D. Kuyucu, Brain connectivity analysis from EEG signals using stable phase-synchronized states during face perception tasks, Physica A **434**, 273 (2015).

[29] V. A. Maksimenko, A. Lüttjohann, V. V. Makarov, M. V. Goremyko, A. A. Koronovskii, V. Nedaivozov, A. E. Runnova, G. van Luijtelaar, A. E. Hramov, and S. Boccaletti, Macroscopic and microscopic spectral properties of brain networks during local and global synchronization, Phys. Rev. E **96**, 012316 (2017).

[30] K. Schiecke, M. Wacker, F. Benninger, M. Feucht, L. Leistritz, and H. Witte, Matching pursuit-based time-variant bispectral analysis and its application to biomedical signals, IEEE Trans. Biomed. Eng. **62**, 1937 (2015).

[31] L. W. Sheppard, V. Vuksanovi, P. McClintock, and A. Stefanovska, Oscillatory dynamics of vasoconstriction and vasodilation identified by time-localized phase coherence, Phys. Med. Biol. **56**, 3583 (2011).

[32] M. Le Van Quyen, J. Foucher, J.-P. Lachaux, E. Rodriguez, A. Lutz, J. Martinerie, and F. J. Varela, Comparison of Hilbert transform and wavelet methods for the analysis of neuronal synchrony, J. Neurosci. Methods **111**, 83 (2001).

[33] V. Sakkalis, Review of advanced techniques for the estimation of brain connectivity measured with EEG/MEG, Comput. Biol. Med. **41**, 1110 (2011).

[34] A. N. Pavlov, A. E. Hramov, A. A. Koronovskii, E. Y. Sitnikova, V. A. Makarov, and A. A. Ovchinnikov, Wavelet analysis in neurodynamics, Phys. Usp. **55**, 845 (2012).

[35] E. Sitnikova, A. E. Hramov, V. Grubov, and A. A. Koronovsky, Time-frequency characteristics and dynamics of sleep spindles in WAG/Rij rats with absence epilepsy, Brain Res. **1543**, 290 (2014).

[36] A. Bandrivskyy, A. Bernjak, P. McClintock, and A. Stefanovska, Wavelet phase coherence analysis: Application to skin temperature and blood flow, Cardiovasc. Eng. **4**, 89 (2004).

[37] S. S. Lodder and M. J. van Putten, Quantification of the adult EEG background pattern, Clin. Neurophysiol. **124**, 228 (2013).

[38] V. V. Makarov, A. E. Hramov, D. V. Kirsanov, V. A. Maksimenko, M. V. Goremyko, A. V. Ivanov, I. A. Yashkov, and S. Boccaletti, Interplay between geo-population factors and hierarchy of cities in multilayer urban networks, Sci. Rep. **7**, 17246 (2017).

[39] N. Langer, A. Pedroni, L. R. Gianotti, J. Hnggi, D. Knoch, and L. Jncke, Functional brain network efficiency predicts intelligence, Human Brain Mapping **33**, 1393 (2012).

[40] M. P. van den Heuvel, C. J. Stam, R. S. Kahn, and H. E. H. Pol, Efficiency of functional brain networks and intellectual performance, J. Neurosci. **29**, 7619 (2009).

[41] K. H. Lee, Y. Y. Choi, J. R. Gray, S. H. Cho, J.-H. Chae, S. Lee, and K. Kim, Neural correlates of superior intelligence: Stronger recruitment of posterior parietal cortex, NeuroImage **29**, 578 (2006).

[42] I. H. Harding, M. Ycel, B. J. Harrison, C. Pantelis, and M. Breakspear, Effective connectivity within the frontoparietal control network differentiates cognitive control and working memory, NeuroImage **106**, 144 (2015).

[43] T. P. Zanto and A. Gazzaley, Fronto-parietal network: Flexible hub of cognitive control, Trends Cognit. Sci. **17**, 602 (2013).

[44] I. Stitt, K. J. Hollensteiner, E. Galindo-Leon, F. Pieper, E. Fiedler, T. Stieglitz, G. Engler, G. Nolte, and A. K. Engel, Dynamic reconfiguration of cortical functional connectivity across brain states, Sci. Rep. **7**, 8797 (2017).

[45] A. Fornito, B. J. Harrison, A. Zalesky, and J. S. Simons, Competitive and cooperative dynamics of large-scale brain functional networks supporting recollection, Proc. Natl. Acad. Sci. USA **109**, 12788 (2012).